

T. KÖNEMANN^{1,✉}
W. BRINKMANN¹
E. GÖKLÜ¹
C. LÄMMERZAHN¹
H. DITTUS¹
T. VAN ZOEST²
E.M. RASEL²
W. ERTMER²
W. LEWOCZKO-ADAMCZYK³
M. SCHIEMANGK³
A. PETERS³
A. VOGEL⁴
G. JOHANNSEN⁴
S. WILDFANG⁴
K. BONGS⁴
K. SENGSTOCK⁴
E. KAJARI⁵
G. NANDI⁵
R. WALSER⁵
W.P. SCHLEICH⁵

A freely falling magneto-optical trap drop tower experiment

¹ ZARM, University of Bremen, Am Fallturm, 28359 Bremen, Germany

² Institute of Quantum Optics, Leibniz University Hannover, Welfengarten 1, 30167 Hannover, Germany

³ Institute of Physics, Humboldt University of Berlin, Hausvogteiplatz 5–7, 10117 Berlin, Germany

⁴ Institute of Laser-Physics, University of Hamburg, Luruper Chaussee 149, 22761 Hamburg, Germany

⁵ Institute of Quantum Physics, University of Ulm, Albert-Einstein-Allee 11, 89069 Ulm, Germany

Received: 30 June 2007/Revised version: 8 October 2007
Published online: 29 November 2007 • © Springer-Verlag 2007

ABSTRACT We experimentally demonstrate the possibility of preparing ultracold atoms in the environment of weightlessness at the earth-bound short-term microgravity laboratory Drop Tower Bremen¹, a facility of ZARM – University of Bremen². Our approach is based on a freely falling magneto-optical trap (MOT) drop tower experiment performed within the ATKAT collaboration (“Atom-Catapult”) as a preliminary part of the QUANTUS pilot project³ (“Quantum Systems in Weightlessness”) pursuing a Bose–Einstein condensate (BEC) in microgravity at the drop tower [1, 2].

Furthermore we give a complete account of the specific drop tower requirements to realize a compact and robust setup for trapping and cooling neutral rubidium ⁸⁷Rb atoms in microgravity conditions. We also present the results of the first realized freely falling MOT and further accomplished experiments during several drops.

The goal of the preliminary ATKAT pilot project is to initiate a basis for extended atom-optical experiments which aim at realizing, observing and investigating ultracold quantum matter in microgravity.

PACS 67.85.-d

1 Introduction

Since the possibility of trapping and cooling neutral atoms, ultracold quantum degenerate gases have shifted boundaries in a growing field of modern physics based on the first observation of Bose–Einstein condensates in 1995 [3, 4] and appreciated by the Nobel Prizes in 1997 and 2001.

The current developments in the domain of atom optics lead to an utilization of ultracold quantum matter techniques in unique practical applications as high-precision atomic clocks, atom interferometer technologies and inertial sensing instruments for gravity field mapping, underground structure detection, autonomous navigation, as well as precision measurements in fundamental physics. These applications relate to many different fields of interests in quantum physics and cross-linked research on earth and in space. On the practical side the expectations of even higher precision measurements can be performed by arbitrarily extending the time of unperturbed evolution of quantum degenerate systems. In respect thereof weightlessness provides an outstanding basis for such applications and measurements. Motivated by these prospects, many national and international groups have initialized research programs aiming for compact, transportable and ruggedly designed atom-optical experiments like PHARAO/ACES [5], PARCS [6], RACE [7], I.C.E. [8], and first initiatives by the ENS group in the early 1990s [9], at JPL and Stanford University, which might be launched in parabolic flights and space applications.

Thanks to an easy access to low gravity on earth, realization of quantum degenerate gases in excellent microgravity conditions at drop towers could open a new kind of perspectives on earth-bound experiments, e.g., to achieve long observation times and unprecedented low temperature regimes. Thus, ultracold quantum matter in an environment of weightlessness represents an emerging area of science in quantum engineering with an impressive potential for a future technology and multidisciplinary applications.

¹ <http://www.zarm.uni-bremen.de/>

² Center of Applied Space Technology and Microgravity

³ <http://www.quantus-projekt.de/>

The Drop Tower Bremen provides a new tool for atom-optical experiments like ATKAT and QUANTUS. The outstanding features of the 146 m (effective free fall 110 m) high drop tower are to generate a quality of weightlessness of 10^{-5} m s^{-2} in the frequency range below 100 Hz for 4.7 s. Its short measuring repetition rate of three times per day is limited by the necessary time to evacuate the drop tube with a volume of about 1700 m^3 . Advances in drop tower performance can be expected soon from the new catapult system, which expands the time of free fall up to approximately 9 s at the same quality of microgravity.

In comparison with parabolic flights, the residual gravitation in the Drop Tower Bremen is about three orders of magnitude better than in the Zero-G Airbus (10^{-5} m s^{-2} compared to 10^{-2} m s^{-2} in the frequency range below 100 Hz). According to financial expenses of atom-optical space-proof experiments on orbital platforms like satellites or the space station, accomplishing drop tower experiments require shorter developmental periods and thus much lower costs.

The ATKAT collaboration displays an excellent precursor for first experimental demonstrations of ultracold trapped atoms in the environment of microgravity at the Drop Tower Bremen. The ATKAT pilot project may be understood as a preliminary drop tower experiment that is closely related to the QUANTUS pilot project. The individual objectives of ATKAT and QUANTUS differ in strategic questions, while ATKAT pretests several expected and unexpected non-laboratory influences on hardware within the drop tower conditions, QUANTUS directly investigates in realizing a BEC in microgravity using the experiences and results of ATKAT.

With ATKAT, we demonstrate a magneto-optical trap in microgravity, which is especially supposed to indicate and sense perturbations like residual magnetic fields inside the drop tower tube, temperature changes inside the completely closed capsule, mechanical vibrations and shocks up to 500 m s^{-2} at deceleration acting on the drop tower experiment.

2 Experimental setup

Obviously, a drop tower experiment demands a compact and robust setup in order to meet the specific requirements of mechanical shock resistance, limited payload mass and volume, and restricted electrical power consumption. Thus, drop tower experimental setup techniques substantially differ from various common laboratory experiments. In the case of an atom-optical experiment like ATKAT designed to trap and cool neutral rubidium ^{87}Rb atoms in drop tower conditions, one has to house all experimental equipments inside of a drop capsule (see Fig. 1), which so far required entire optical tables in a laboratory.

The Drop Tower Bremen standard capsule has a total height of 2.86 m and an effective payload height of about 1.73 m. Each insertable capsule platform allocates a diameter of 0.6 m for one part of the experimental equipment. Finally, the absolute required platform amounts are specified by the respective used experiments or effective capsule payload height. However, the sum of all experimental equipments are limited by a mass of 234 kg shared in a maximum available volume of less than 0.5 m^3 .

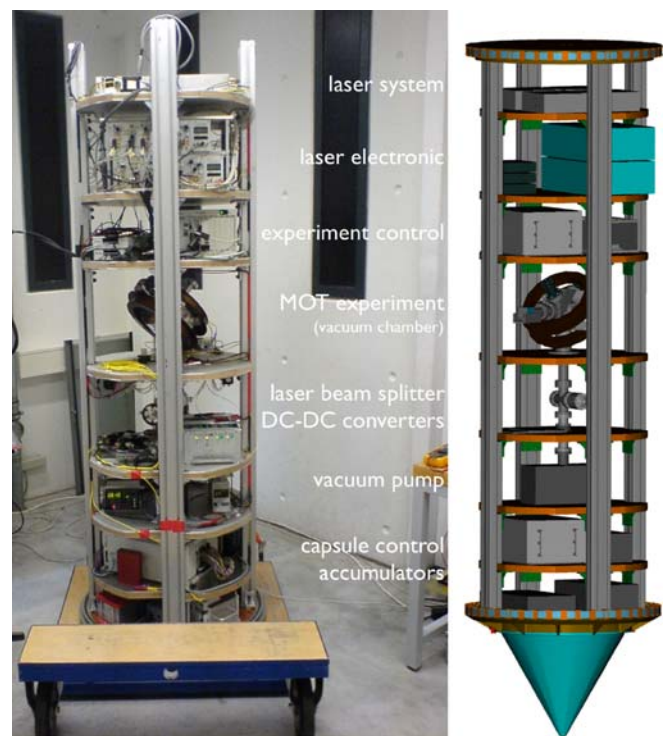


FIGURE 1 ATKAT drop capsule setup without magnetic shield around the MOT vacuum chamber

2.1 Magneto-optical trap setup

Due to environmental conditions, the ATKAT magneto-optical trap setup is based on a small-sized vacuum chamber made of a rigid aluminium block shaped like a honeycomb cell form (see Fig. 2). In order to withstand acceleration forces up to 250 kN during the capsule deceleration, vacuum glass cell techniques are not the first choice in such experiments. The various sealing methods used in the aluminium vacuum chamber and the performance of the pressure stability test will be discussed in detail in Sect. 3.1.

We utilize four laser beam ports for a three-dimensional mirror MOT, at which two beams are reflected by a 45° -mirror inside the chamber. The four laser beams transmitted to the vacuum chamber via polarization-maintaining optical fibers are expanded to a diameter of 20 mm and collimated by telescope lenses for a wide and homogeneous cooling field. In addition, all telescopes rigidly attached to the body of the vacuum chamber are equipped with retarding waveplates.

A pair of air-cooled anti-Helmholtz coils producing the magnetic field gradient of 9.26 G cm^{-1} along the coil axis in the middle of the chamber and three supplemental pairs of smaller Helmholtz coils compensating external magnetic fields are mounted outside of the vacuum chamber.

The ^{87}Rb magneto-optical trap is directly loaded from the rubidium background gas. A commercially available current-controlled dispenser⁴ releases the rubidium atoms into the chamber from the top flange, which is cable-connected on two electrical vacuum stable feedthroughs. We are currently able to trap and cool approximately 10^7 to 10^8 neutral ^{87}Rb atoms,

⁴ SAES getters

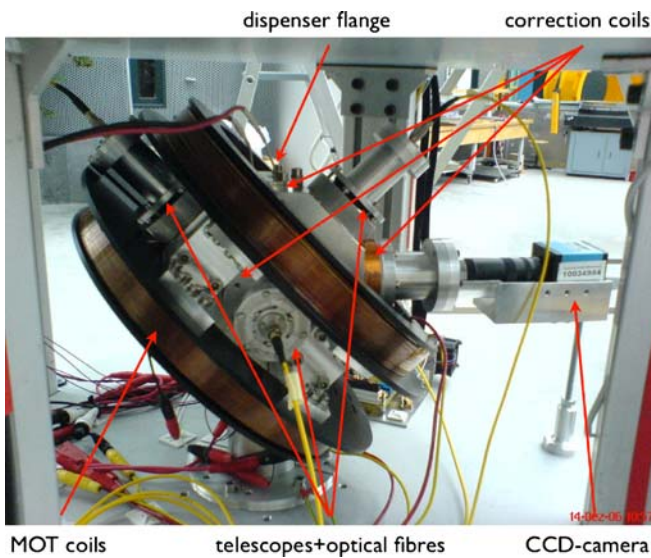


FIGURE 2 ATKAT magneto-optical trap setup without magnetic shield

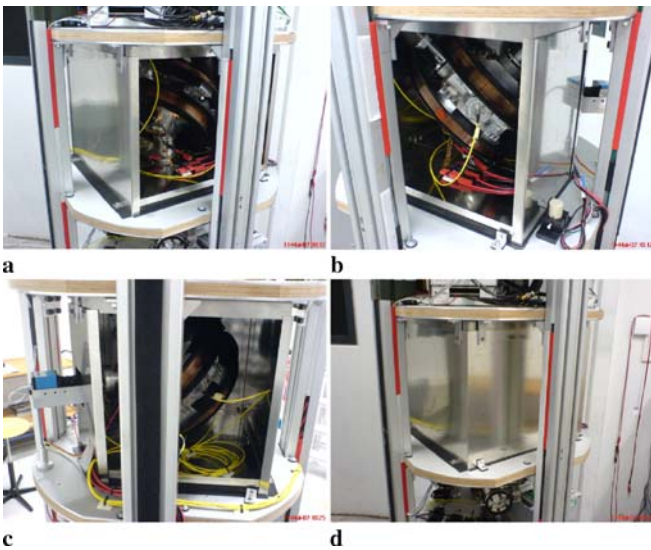


FIGURE 3 (a,b) View of front-side opened magnetic shield. (c) View of back-side opened magnetic shield and left-side CCD-camera. (d) Fully closed μ -metal shield around the MOT vacuum chamber

depending on the chosen dispenser current in drop mode. The emitted fluorescence light from the trapped atoms is recorded by a CCD-camera at 30 frames/s during the drop experiment.

After monitoring the expected recurring changes of the magnetic field inside the drop tower tube, which are strongly acting on the freely falling MOT position, a μ -metal shield with a wall thickness of 1 mm and a permeability of approx. 30 000 was later installed around the MOT vacuum chamber as shown in Fig. 3a–d to shield external magnetic influences.

A detailed description of the magnetic and otherwise drop tower conditions will be represented in the results in Sect. 3.

2.2 Laser system and laser electronics

Stable frequency and intensity of light are crucial for the performance of a magneto-optical trap [10]. Thus, in constructing a reliable and robust laser system capable of operating at the drop tower, one has to consider some nontypical

laboratory conditions. In particular, temperature increases inside the drop capsule after 2 h of drop tube evacuation and there are critical vibrations of the capsule platforms at the moment of capsule release as mechanical stress is relaxing. This must not cause changes in laser light intensity and frequency.

For magneto-optical cooling of rubidium, a few tens of milliwatts of 780 nm laser power is needed with a linewidth smaller than the natural width of the $^{87}\text{Rb}-D_2$ transition, $\Gamma \approx 6$ MHz. For the sake of mechanical stability, we have intentionally refrained from using extended cavity diode lasers (ECDL), which are the most common choice for laser cooling. Instead, we utilize distributed feedback (DFB) laser diodes with an intrinsic grating in the active semiconductor area [11]. In contrast to an ECDL, a DFB diode has a very high intrinsic stability. Furthermore, it has an extremely wide mode-hop-free operation range of more than 100 GHz, which greatly facilitates its use. However, its emission linewidth is wider than that of an ECDL, but with 1–3 MHz it is still comparable with the natural linewidth and assures effective cooling.

Our laser system is schematically shown in Fig. 4a. It consists of two DFB master lasers stabilized to atomic transitions, a master oscillator power amplifier (MOPA) module including a DFB laser and tapered amplifier diode, a beat module, and a power distribution module. The first master laser is based on a Doppler-free dichroic atomic vapor laser lock (DFDL) technique [12] and provides approximately 4 mW of light for the repumping transition in the cooling cycle (servo bandwidth: 15 kHz). The second one utilizes modulation transfer spectroscopy (MTS) lock [13, 14] and serves as a reliable frequency reference for the cooling transition (modulation frequency: 8.1 MHz, servo bandwidth: 70 kHz). The MOPA is offset-locked to the MTS master laser and its tapered amplifier supplies the required 100 mW of trapping light after coupling into the fiber guiding the light from the MOPA module to the beam power splitting module, where the trapping and repumping beams are superimposed, split into four beams of equal power (approx. 15 mW of trapping light) and coupled into four fibers guiding the superimposed light to the telescopes of the vacuum chamber.

All mounts for the standard optic components at a beam height of 20 mm in the laser modules are self designed with a special emphasis on mechanical stability. The lasers and optics including stabilization with rubidium spectroscopy cell are positioned in robust housings of only $210 \times 190 \times 60$ mm³ (see Fig. 4b)), which are made of stress-free aluminum with a wall thickness of 10 mm. The whole system, including electronics, fits the area of two platforms in the drop capsule setup as shown in Fig. 1. Note also that all modules are interlinked with optical fibers, which enhances flexibility of use.

For the power-splitting module mentioned above, we utilize a commercially available module.⁵ Additionally, the optical power of the two input beams is monitored with a pair of built-in photodiodes.

2.3 Capsule power supply and control system

In order to supply the electrical capsule power, a series of lead accumulators are permanently integrated as

⁵ Schäfer+Kirchhoff GmbH “Fibre Port Cluster 2 to 4”

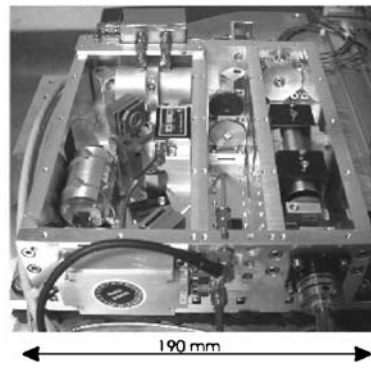
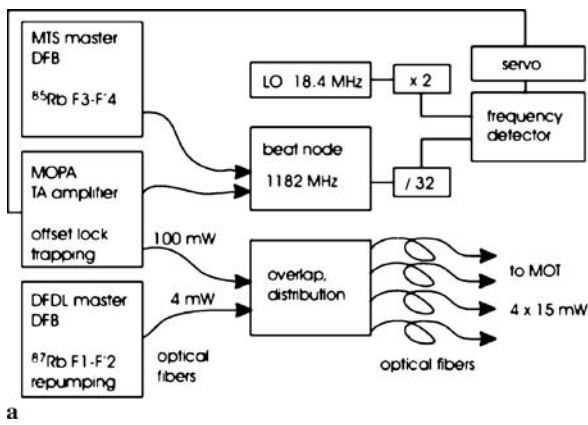


FIGURE 4 (a) Schema of the compact laser system. (b) Modulation transfer spectroscopy master laser in robust stress-free aluminum chassis

standard equipment at the very bottom platform of the drop capsule. They provide a nominal 28 V dc voltage over six computer controllable current channels to the drop experiment. The applicable maximum current is 40 A per channel and hence the complete power consumption of the capsule experiment is limited by 1.12 kW. All lead accumulators are constantly buffered by an external battery charger, which is only disconnected about 1 min prior to the drop command. The available energy usable during the drop is about 0.7 kW while the experiment is running.

A compact PXI computer with a real-time operating system⁶ is installed above the accumulator platform, which can be controlled by a wireless local area network (WLAN) communication system. The capsule control system is used to exchange data between the control center of the drop tower facility and the drop capsule and to give remote-controlled commands to completely handle the drop experiment. All received experimental data can be immediately monitored on the control center screens and is securely recorded on base servers.

3 Results

3.1 Vacuum stability test

In order to minimize collision rates between cold and residual background atoms, it is required that an ultra high vacuum (UHV) in any atom-optical experiment be achieved. Up till now, UHV chamber drops have not been carried out at the drop tower before in the ATKAT pilot project. As a critical aspect, our UHV chamber has to pass the deceleration phase for several drops within a campaign (19 times so far). Thus, the vacuum chamber itself and the vacuum gasket techniques have to be chosen as stable as possible.

We utilize standard and non-standard vacuum gasket techniques realizing an UHV inside our vacuum chamber to test a wide field of sealing opportunities at once. Additionally, we operate with a special drop tower “*VacIon Plus 40 Diode*” ion getter pump modified and specified by Varian, as well as with a commercial cold cathode gauge system for in situ pressure sensing.

Our vacuum chamber is made of a small aluminium block, at which standard CF vacuum gasket techniques fail because the material is too soft. Instead, we use lead gaskets for harder

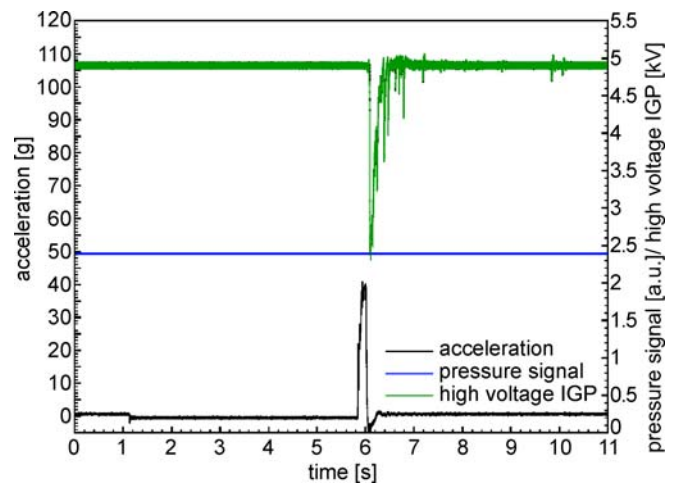


FIGURE 5 Drop result of a stability test of ATKAT vacuum chamber utilizing standard and non-standard vacuum gasket techniques

non-standard vacuum chamber ports, e.g., at the dispenser flange, and softer indium gaskets for the sensitive BK7 glass windows. Each lead or indium gasket with a thickness of 2.0 mm and 0.5 mm, respectively, is formed to a ring and squeezed between the corresponding vacuum components.

The constant blue line curve in Fig. 5 represents the leak tightness of the ATKAT vacuum chamber in a vacuum stability drop experiment, which is directly read out from the cold cathode gauge controller corresponding to an UHV pressure of 1.8×10^{-10} mbar. Although the high voltage at the ion getter pump displayed in the green curve shortly collapses from 5 kV to 2.5 kV for about half a second during the deceleration phase, the pressure inside the vacuum chamber stays constant. The deceleration phase monitored on this drop experiment has a temporary peak acceleration of about 400 m s^{-2} as shown by the black curve. Each of the acceleration curves is measured by a standard built-in sensor of the drop capsule.⁷

3.2 Laser stability test

As already mentioned, stable laser frequency and power are important for efficient cooling. So far we have performed several dedicated drop tower tests of the laser system. We recorded the frequency error signals and the light intensity

⁶ National Instruments Corporation

⁷ ZARM Drop Tower User Manual

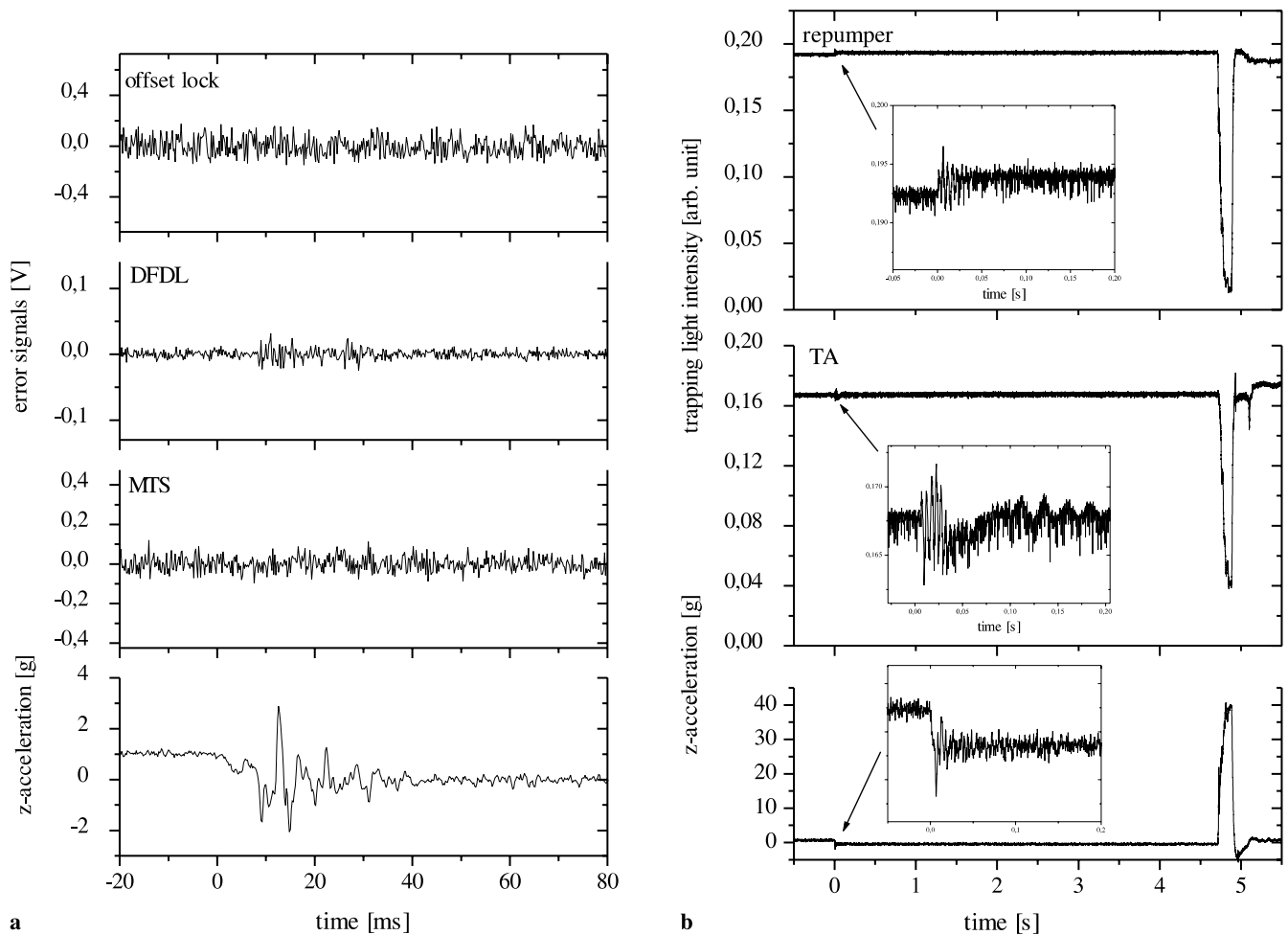


FIGURE 6 (a) Error signals of the three laser locks show no change in the laser frequency during the capsule release. (b) Intensity of the laser light at the input ports of the beam power splitting module during the flight

during each drop of the freely falling MOT. Error signals of the three lasers at the moment of drop capsule release are displayed in Fig. 6a. No significant frequency change has been monitored, which indicates a good performance of the laser lock loops. Figure 6b shows the intensity of the trapping and repumping beams at the input ports 1 and 2 of the beam power splitting module during the whole flight. A little acceptable jitter of about 3% of the total intensity can be observed at the moment of the capsule release. Both intensities stay stable during the drop and vary by typically no more than 10% after the impact, so that fiber coupling has to be only slightly readjusted after the capsule recovery. The intensity of the superimposed beams at the four output ports of the beam power splitting module is not directly monitored so far, it will be later investigated by a special measurement module in catapult flights.

Until now we have not utilized any active stabilization system for the optical power and we simply rely on the mechanical stability of our laser setup. Note also that possible temperature increases of about 6 °C inside the drop capsule between laboratory operation and drop release did not have a negative effect on the performance of the laser system stability and the MOT preparation at the top of the drop tube before the experiment launch.

3.3 Ultracold trapped atoms in microgravity

Since the beginning of trapping and cooling of neutral atoms in the early 1980s, magneto-optical traps have been an initial state for a multiplicity of experiments generating ultracold quantum degenerate gases and Bose–Einstein condensates in laboratories. Today there are only a limited number of compact and transportable atom-optical setups and realized experiments.

The demonstration of a freely falling MOT in drop tower operations is to initiate a first access to a new class of compact and robust atom-optical experiments in microgravity conditions.

3.3.1 A freely falling MOT. At the end of 2006, a first ^{87}Rb magneto-optical trap within the ATKAT pilot project could be experimentally demonstrated in an environment of microgravity at the Drop Tower Bremen. Besides the aspects of pretesting the vacuum and laser stability as mentioned in Sects. 3.1 and 3.2, recurring changes of the magnetic field inside the drop tower were observed and are due to the fact that the vacuum drop tube is manufactured from 6 m high solid steel tube parts with constant but different injected residual magnetic remanences of the order of the terrestrial magnetic

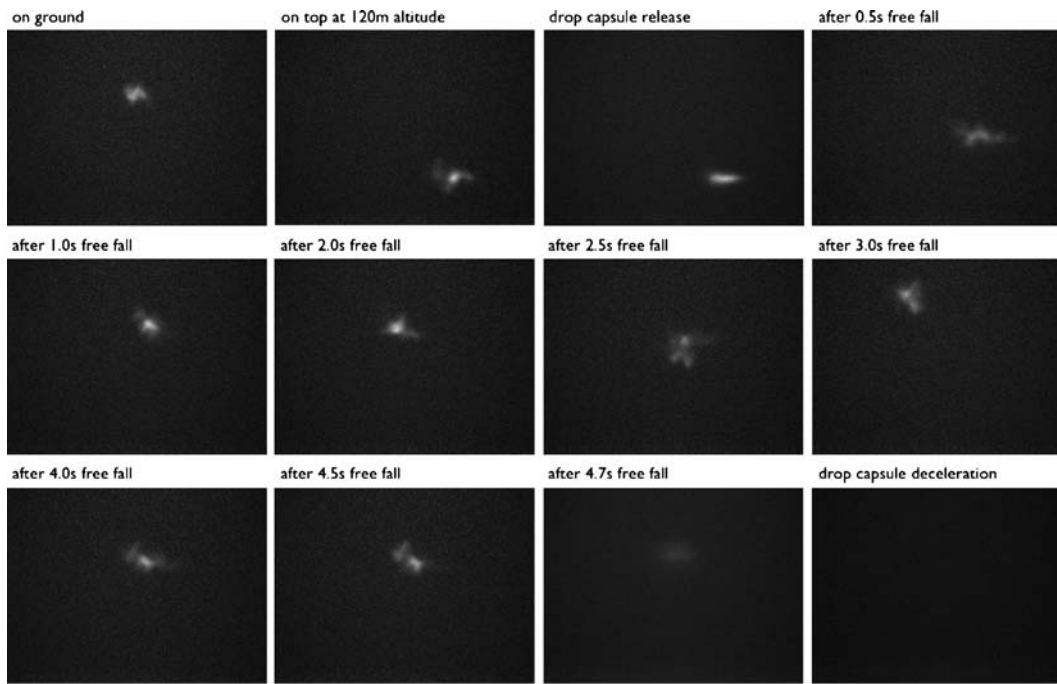
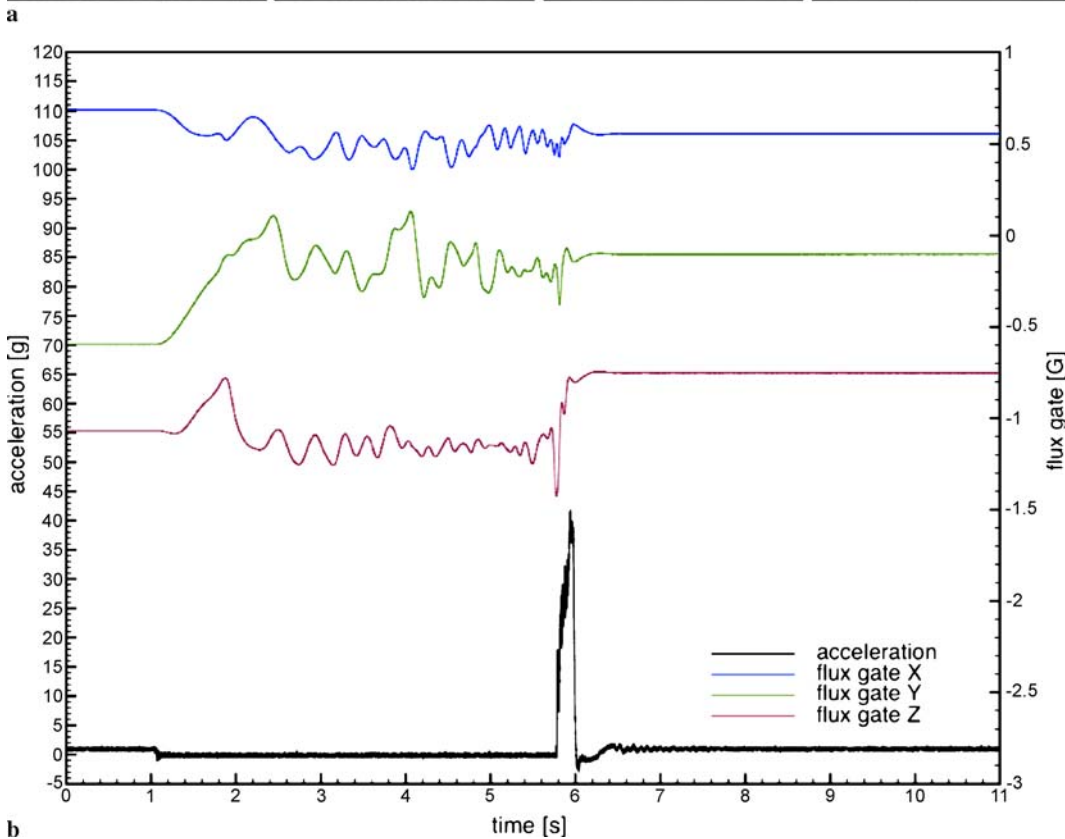


FIGURE 7 (a) Chronological excerpt from the non-shielded freely falling ^{87}Rb magneto-optical trap including the effect of residual magnetic fields at the Drop Tower Bremen (CCD-chip size: 5.80 mm (h) \times 4.92 mm (v)). After 4.7 s of free fall the laser beam powers collapse during the beginning of the deceleration phase and in the following the lasers are unlocked at the impact. **(b)** Three-dimensional flux gate measurement at the MOT vacuum chamber during a drop without MOT operation and magnetic shield



field. In addition, some technical drop tower equipment induces several constant or low-frequency magnetic fields at the drop tube top, e.g., tower winch, drop regulation mechanics and electronics.

For a typical magnetic field gradient of several Gauss per centimeter produced by the heavy MOT coils, the field minimum (and thus the position of an atomic cloud) are shifted a couple of millimeters due to external magnetic fields. In

respect thereof, the expected effect of the residual magnetic fields inside the drop tube measured by a three-dimensional flux gate⁸ (see Fig. 7b) is represented on the non-shielded freely falling MOT in Fig. 7a. In this case, the chosen currents of the three compensation coil pairs were adjusted and fixed to select the right MOT position for the CCD-chip on top of

⁸ Stefan Mayer Instruments “FLC3-70”

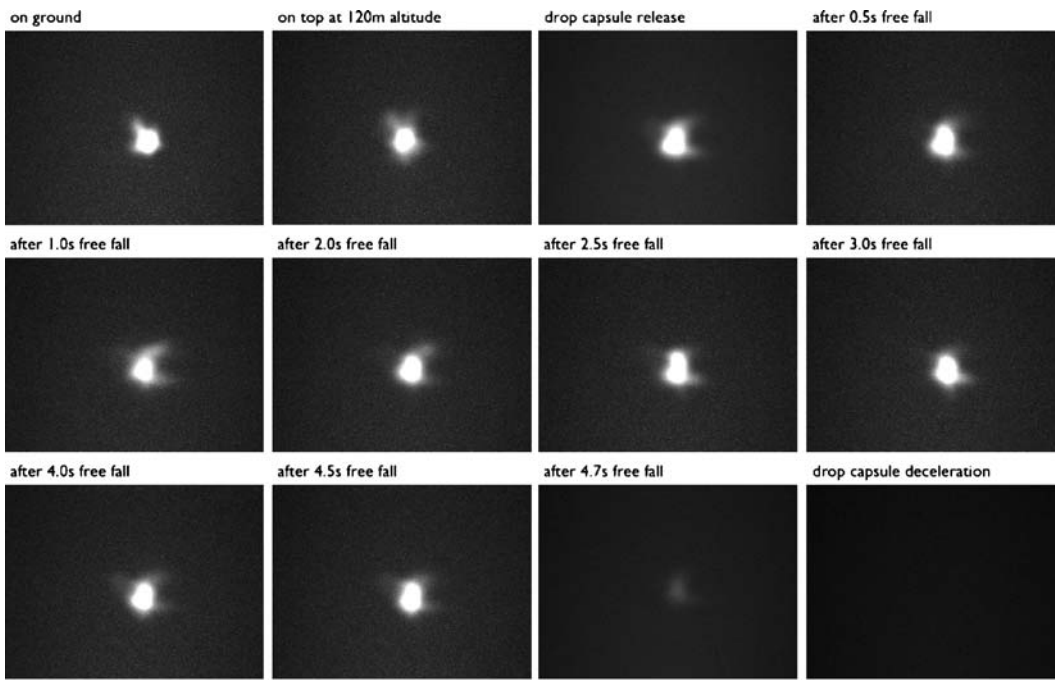
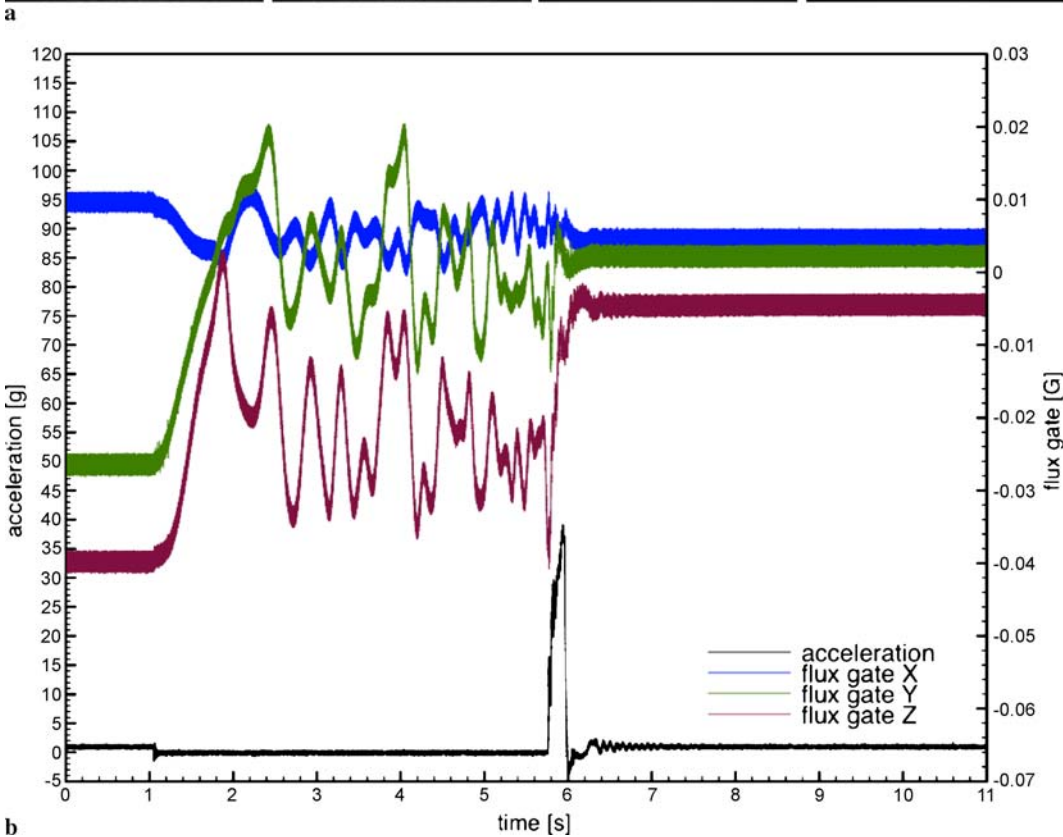


FIGURE 8 (a) Chronological excerpt from a magnetic shielded ^{87}Rb magneto-optical trap during the free fall at the Drop Tower Bremen (CCD-chip size: 5.80 mm (h) \times 4.92 mm (v)). After 4.7 s of free fall one observes the same like in Fig. 7a. (b) Three-dimensional flux gate measurement at the μ -metal shielded MOT vacuum chamber during a drop without MOT operation



the drop tube during MOT operation shortly before the drop release.

The three-dimensional high sensitive flux gate sensor is directly positioned next to the vacuum chamber on the same capsule platform (refer Figs. 1 and 2), at which the X -direction indicates the CCD-camera view axis, the Y -direction is perpendicularly coplanar with it and the Z -direction describes the vertical drop capsule axis. All flux

gate data was recorded in separate flights with magnetic coils switched off not to saturate the flux gate sensor.

3.3.2 A magnetically shielded MOT in free fall. After the first drop campaigns our μ -metal shield was available to be installed around the MOT vacuum chamber as displayed in Fig. 3a–d to shield all kind of external magnetic influences. The effect of the magnetic shield on the freely falling

magneto-optical trap is clearly visible in the stable MOT position (see Fig. 8a). Therefore we adjusted and fixed the currents of the compensation coils once to center the MOT position in laboratory, so we did not readjust for the flights again. Nevertheless, the three-dimensional flux gate sensor now positioned inside the μ -metal shield measures some non-shielded residual magnetic fields as shown in Fig. 8b. In order to compare the measurements with and without the μ -metal shield (refer Figs. 7b and 8b) the flux gate sensor position was chosen to be the same. It allows to observe a reduction of the magnetic flux density from 0.69 G to 0.01 G in X -direction, from 0.59 G to 0.03 G in Y -direction and from 1.07 G to 0.04 G in Z -direction on top of the drop tube. During and after the deceleration phase, the drop capsule is inside the deceleration container, which is manufactured from solid steel. Thus, the measured magnetic flux densities decrease again.

Now we are able to calculate an effective shielding factor for all three monitored axis during the whole flight. The effective shielding factors depend on the specific μ -metal shield geometry, which differs in each spatial direction. The factors range from about 20 on the Y -axis, to over 27 on the Z -axis, and up to 69 on the X -axis. After securely passing several shocks up to 400 to 500 m s⁻² in nine drops, the μ -metal shield has not varied from its shielding factor on any axis so far.

Finally, proper compensation of the residual magnetic fields inside the drop tube is very important for polarization-gradient cooling in optical molasses, which is going to be tested in subsequent drop experiments.

4 Conclusions

In summary, we present the experimental demonstration of a non-shielded and magnetically shielded magneto-optical trap in the environment of microgravity at the earth-bound laboratory Drop Tower Bremen performed within the ATKAT collaboration. Furthermore, we discussed the realization of our experimental drop capsule setup, in particular the leak tightness of the vacuum chamber and the stability of the laser system.

The utilized atom-optical drop capsule setup did not reveal any structural weak points not passing the specific drop tower requirements after 19 drops, so far. Consequentially, it was possible to realize a very compact and robust setup

for trapping and cooling neutral rubidium ⁸⁷Rb atoms in microgravity conditions initiating positive prospects for further atom-optical experiments in microgravity.

The amount of obtained experiences will have a relevant meaning in the near future to use the ATKAT drop capsule equipment in the drop tower catapult system, and to promise a successful implementation of the QUANTUS pilot project pursuing a Bose–Einstein condensation drop experiment in microgravity at the drop tower.

ACKNOWLEDGEMENTS The ATKAT pilot project gratefully acknowledges the support from the German Aerospace Center (Deutsches Zentrum für Luft- und Raumfahrt e.V. – DLR) under the project number DLR 50 WM 0508. We also thank the EADS Astrium for providing us the drop tower specified ion getter pump.

REFERENCES

- 1 A. Vogel, M. Schmidt, K. Sengstock, K. Bongs, W. Lewoczko, T. Schuldt, A. Peters, T. van Zoest, W. Ertmer, E.M. Rasel, T. Steinmetz, J. Reichel, T. Könemann, W. Brinkmann, E. Göklü, C. Lämmerzahl, H. Dittus, G. Nandi, R. Walser, W.P. Schleich, *Appl. Phys. B* **84**, 663 (2006)
- 2 G. Nandi, R. Walser, E. Kajari, W.P. Schleich, arXiv:cond-mat/0610637v1 (2006)
- 3 M.H. Anderson, J.R. Ensher, M.R. Matthews, C.E. Wieman, E.A. Cornell, *Science* **269**, 198 (1995)
- 4 K.B. Davis, M.-O. Mewes, M.R. Andrews, N.J. van Druten, D.S. Durfee, D.M. Kurn, W. Ketterle, *Phys. Rev. Lett.* **75**, 3969 (1995)
- 5 P. Laurent, P. Lemonde, E. Simon, G. Santorelli, A. Clairon, N. Dimarcq, P. Petit, C. Audoin, C. Salomon, *Eur. Phys. J. D* **3**, 201 (1998)
- 6 S.R. Jefferts, T.P. Heavner, L.W. Hollberg, J. Kitching, D.M. Meekhof, T.E. Parker, W. Phillips, S. Rolston, H.G. Robinson, J.H. Shirley, D.B. Sullivan, F.L. Walls, N. Ashby, W.M. Klipstein, L. Maleki, D. Seidel, R. Thompson, S. Wu, L. Young, R.F.C. Vessot, A. De Marchi, *Joint Meet. Eur. Freq. Time Forum and The IEEE Int. Freq. Contr. Symp.*, Besançon, France, April (1999), pp. 141–144
- 7 C. Fertig, K. Gibble, *IEEE/EIA Int. Freq. Contr. Symp.*, Kansas City, MO, June (2000), pp. 676–679
- 8 G. Varoquaux, N. Zahzam, W. Chaibi, J. Clément, O. Carraz, J. Brantut, R.A. Nyman, F.P. Dos Santos, L. Mondin, M. Rouzé, Y. Bidet, A. Bresson, A. Landragin, P. Bouyer, arXiv:0705.2922v2 (2007)
- 9 B. Lounis, J. Reichel, C. Salomon, *CR Acad. Sci.* **316**, 739 (1993)
- 10 H.J. Metcalf, P. van der Straten, *Laser Cooling and Trapping* (Springer, Berlin Heidelberg New York, 1999)
- 11 J.E. Carroll, J.E.A. Whiteaway, R.G.S. Plumb, D. Plumb, *Distributed Feedback Semiconductor Lasers* (IEE, Redwood Books, Trowbridge, NJ, 1998)
- 12 G. Wasik, W. Gawlik, J. Zachorowski, W. Zawadzki, *Appl. Phys. B* **75**, 613 (2002)
- 13 J.H. Shirley, *Opt. Lett.* **7**, 537 (1982)
- 14 J. Zhang, D. Wei, C. Xie, K. Peng, *Opt. Express* **11**, 1338 (2003)